

9. Chondrites are primitive meteorites that contain small spherules, called chondrules, and appear to have been produced very early in the formation of the solar system. The C1 chondrites are the most primitive, and chemical data are commonly normalized to their composition.
10. Pallasites and mesosiderites are stony iron meteorites consisting of silicate masses contained in a matrix of Fe-Ni metal. Pallasites are considered to have comprised the boundary between the core and the mantle of asteroid bodies.
11. Basaltic achondrites (collectively called HED) are stony meteorites that have undergone complex igneous histories; eucrites bear a resemblance to terrestrial basalt lavas.
12. R. Clayton, *Annu. Rev. Earth Planet. Sci.* **21**, 115 (1993).
13. T. Bunch *et al.*, *Contrib. Mineral. Petrol.* **25**, 297 (1970).
14. Siderophile elements are those that alloy in Fe-Ni metal.
15. B.-G. Choi *et al.*, *Geochim. Cosmochim. Acta* **59**, 593 (1995).
16. A. Kracher, *Proc. Lunar Planet. Sci. Conf.* **15**, C689 (1985).
17. A. Meibom *et al.*, *Meteoritics* **30**, 544 (1995).
18. V. F. Buchwald, *Handbook of Iron Meteorites* (Univ. of California Press, Berkeley, 1975).
19. Cohenite is an Fe-Ni carbide mineral.
20. The REE content of olivine is so low that its contribution to the whole rock composition is negligible.
21. We thank J. T. Wasson for analyzing this PDZ metal to confirm its IIIA classification, E. R. D. Scott for a helpful discussion, R. Schmitt for a noble attempt to analyze a vanishingly small flake of PDZ, and two anonymous referees who added stimulating ideas and improved this report immeasurably. This work was supported by NASA grants NAGW-3569 (E.J.O.), NAGW-3384 (A.M.D.), and NAGW 3416 (I.M.S.) and NSF grants EAR 92-18857 (R.N.C.), EAR-9303530 (I.M.S.), and EAR-9316062 (I.M.S.).

21 May 1996; accepted 18 July 1996

Radiocarbon in Hydrologic Systems Containing Dissolved Magmatic Carbon Dioxide

Timothy P. Rose* and M. Lee Davisson

In regions of active volcanism, the presence of magmatic carbon dioxide (CO₂) in regional hydrologic systems provides a radiocarbon-depleted tracer for delineating ground-water transport and mixing processes and provides a means of assessing regional magmatic carbon fluxes. Variations in the stable carbon isotopic composition ($\delta^{13}\text{C}$) and carbon-14 values of springs and surface waters from the southern Cascade Range show consistent patterns of carbon isotopic mixing between magmatic, biogenic, and atmospheric CO₂ reservoirs. Radiocarbon measurements of waters from the Lassen region in northern California were used to construct a ground-water carbon-14 contour map, revealing principal subsurface flow paths and a broad region of diffuse magmatic CO₂ flux.

Recent soil gas studies have shown that large quantities of magmatic CO₂ are released as diffuse emissions from the flanks of some active volcanoes (1). In many cases, the CO₂ must percolate through a thick section of water-saturated bedrock on its way to the surface, raising the question of how much of the total CO₂ flux is removed by dissolution in ground water. If the quantity of dissolved CO₂ is characteristically large relative to the diffuse or geothermal gas flux, it may have implications for estimates of the global volcanic CO₂ flux (2) or studies of catastrophic CO₂-degassing events (3). Because magmatic CO₂ ordinarily contains no ¹⁴C, the measurement of ground-water ¹⁴C activities in volcanically active regions may provide a means of addressing this question. We describe here results from a regional ¹⁴C hydrologic survey in the southern Cascade Range of California and Oregon.

We collected about 40 water samples from springs and spring-fed creeks in the southern Cascades during 1994 and 1995,

more than half of which were from the Lassen region (Fig. 1). Dissolved inorganic carbon (DIC) extracted from these samples (4) was analyzed for ¹⁴C and $\delta^{13}\text{C}$ (5). Graphical variations in ¹⁴C versus $\delta^{13}\text{C}$ values (Figs. 2 and 3) reveal similar isotope mixing patterns in each volcanic system. We identified three DIC end members, with isotopic compositions represented in Fig. 2 by shaded boxes: (i) DIC in equilibrium with biogenic soil CO₂ [with $\delta^{13}\text{C}_{\text{DIC}}$ near -18 per mil relative to the Pee Dee belemnite (PDB) standard and ¹⁴C \geq 100% modern carbon (PMC)]; (ii) DIC in equilibrium with atmospheric CO₂ [$\delta^{13}\text{C}_{\text{DIC}}$ near 0 per mil, ¹⁴C \geq 100 PMC]; and (iii) DIC in equilibrium with magmatic CO₂ [¹⁴C = 0 PMC]. Carbonate rock is absent in the study areas.

Dissolved inorganic carbon of magmatic origin can show a range in $\delta^{13}\text{C}$ values that depends on the initial composition of the CO₂ gas and on the temperature and pH conditions during CO₂-DIC equilibration (6). In the Lassen region, magmatic DIC-enriched fluids (with ¹⁴C \leq 1 PMC) were observed only in bicarbonate (HCO₃⁻) hot springs (temperature $T = 60^\circ$ to 80°C ; pH = 6.4). The $\delta^{13}\text{C}$ values of these springs

(-5.7 to -7.0 per mil) are consistent with the results that would be obtained as a result of high-temperature isotopic equilibration with CO₂ gas from the Lassen geothermal system ($\delta^{13}\text{C} = -7.5$ to -10.5 per mil; average value = -9.5 per mil) (7). Lower temperature (10°C) equilibration with Lassen geothermal CO₂ could yield $\delta^{13}\text{C}_{\text{DIC}}$ values as enriched as 0 per mil (shaded box in Fig. 2).

At other Cascade volcanic centers, fluids with negligible ¹⁴C activity were observed only in low-temperature, CO₂-rich soda springs (8). Soda spring $\delta^{13}\text{C}$ values ranged from -11.7 to -7.3 per mil and showed an increase in pH from 4.5 to 6.4 that is concomitant with increasing $\delta^{13}\text{C}$ values (Fig. 3).

The $\delta^{13}\text{C}$ -¹⁴C data from the Lassen region define three distinct mixing arrays, represented by linear trends in Fig. 2, all with a common origin at the biogenic DIC end member. Large springs (flow $> 0.3 \text{ m}^3 \text{ s}^{-1}$) generally have lower ¹⁴C values relative to smaller springs, implying a deeper, regional ground-water flow path (9) with a higher probability for interaction with magmatic CO₂. Simple mixing of ground waters containing biogenic DIC with waters similar in composition to the HCO₃⁻ hot springs produced the "dead carbon addition" mixing line of Fig. 2. The exceptional linearity of the data along this trend suggests mixing with magmatic DIC equilibrated over a limited range of temperature and pH conditions.

A second mixing line in Fig. 2 is defined by the interaction of waters containing biogenic DIC with waters that recharge in the Lassen Peak region. The latter is characterized by surface water from Lost Creek, which originates from springs on the poorly vegetated north slope of Lassen Peak and has a $\delta^{13}\text{C}$ value that indicates low-temperature equilibration with a mixture of magmatic and atmospheric CO₂ gases. Winter snowfall in this region averages $>2.3 \text{ m}$ of

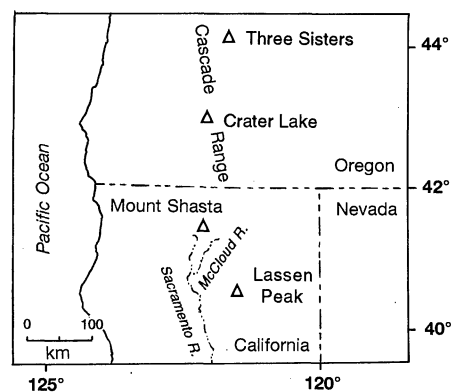


Fig. 1. Map showing locations of major volcanic centers and rivers discussed in the text.

Isotope Sciences Division, L-231, Lawrence Livermore National Laboratory, Livermore, CA 94550, USA.

*To whom correspondence should be addressed.

Table 1. Dissolved magmatic carbon fluxes.

Sample	Discharge (m ³ s ⁻¹)	Temperature (°C)	pH	DIC (×10 ⁻² kg m ⁻³ HCO ₃ ⁻)	δ ¹³ C (per mil)	¹⁴ C (PMC)	Fraction magmatic DIC	Magmatic DIC flux (kg year ⁻¹)
<i>Lassen volcanic center</i>								
Rising River Springs	8.5	8	7.3	5.2	-9.1	79	0.28	3.9 × 10 ⁶
Crystal Lake Springs	2.8	10	8.2	5.6	-12.5	83	0.25	1.2 × 10 ⁶
Big Spring	3.5	8	6.9	8.0	-10.5	44	0.60	5.3 × 10 ⁶
Hat Creek	0.4	4	7.3	2.5	-7.6	73	0.34	1.2 × 10 ⁵
Total								1.1 × 10 ⁷
<i>Mount Shasta volcanic center</i>								
Sacramento River near Dunsuir								
Base flow (August 1994)	6.5	14	8.4	6.6	-6.5	70	0.36	4.9 × 10 ⁶
Runoff (June 1995)	21.8	12	6.8	4.9	-6.1	95	0.13	4.5 × 10 ⁶
Average								4.7 × 10 ⁶
McCloud River near McCloud	22.4	13	7.5	6.0	-17.4	92	0.17	7.1 × 10 ⁶
Base flow (August 1994)								
Big springs of McCloud River		7	7.5	6.2	-17.4	90	0.18	
Total								1.2 × 10 ⁷

rainfall equivalent per year (10), providing a seasonal blanket that can trap and concentrate diffuse magmatic CO₂ emanations (11). During spring melting, magmatic CO₂ in the soil zone can dissolve in the downward percolating snowmelt and mix with atmospheric CO₂ trapped in the snowpack. Silicate hydrolysis reactions neutralize the pH, resulting in ground water with a DIC composition like that of Lost Creek. The largest cold springs in the Lassen region, Rising River Springs (8.5 m³ s⁻¹), have a δ¹³C-¹⁴C pair that plots on this mixing line (Fig. 2) and a δ¹⁸O value that reflects recharge in the Lassen Peak region (12).

The effect of atmospheric equilibration on waters containing biogenic DIC is represented by the zero-slope mixing line between the biogenic and atmospheric DIC end-members in Fig. 2. Most of the samples on this trend are from low-volume springs with bomb pulse ¹⁴C values (13), representing shallow, localized ground-water flow paths. Because atmospheric CO₂ has a δ¹³C value near -8 per mil (14), a HCO₃⁻ solution that has completely equilibrated

with the atmosphere at 15°C will have a δ¹³C value near +1 (6).

Carbon isotope variations similar to those of the Lassen region are observed in waters throughout the southern Cascade Range (Fig. 3), including the Mount Shasta, Crater Lake, and Three Sisters regions (see Fig. 1). Most of the data in Fig. 3 are from large springs, with additional samples from alpine creeks and soda springs. Two subparallel mixing trends are shown between the inferred biogenic and magmatic DIC end-members, one for Mount Shasta and the other for Oregon (Fig. 3). In each case, the ¹⁴C-depleted magmatic component is represented by CO₂-rich soda springs. The ¹³C enrichment in the Oregon data relative to the Mount Shasta data may reflect higher δ¹³C values in the Oregon soda springs, more ¹³C-enriched biogenic DIC values, or the influence of partial atmospheric equilibration of the biogenic DIC source.

Alpine creeks from the Mount Shasta and the Three Sisters regions show an impressive degree of δ¹³C enrichment as a

result of equilibration with atmospheric CO₂ (Fig. 3). These samples represent late summer snowmelt from high alpine regions. The modern ¹⁴C values of the creeks suggest that little magmatic CO₂ escapes from the high slopes of these volcanoes. If a significant alpine magmatic CO₂ flux were present, these creeks would have C isotope values similar to those of Lost Creek at Lassen (Fig. 2).

The Lassen volcanic center, unlike other active Cascade volcanoes, hosts a well-developed geothermal system with numerous surface discharge features (7, 15, 16). Recent volcanism at the Lassen region is characterized by silicic dome emplacement, including the dacite dome of Lassen Peak (17). Degassing of CO₂ from the shallow, silicic magma chamber beneath Lassen Peak gives rise to a high CO₂ flux on the flanks of the volcano, as indicated by the low ¹⁴C values of spring waters originating on Lassen Peak (Lost Creek) and the pres-

Fig. 2. Variations in ¹⁴C versus δ¹³C values of DIC in waters from the Lassen region. Lines identify important mixing processes involving biogenic, atmospheric, and magmatic DIC end-members (shaded boxes). Bicarbonate hot springs represent magmatic DIC equilibrated at higher temperatures. The average composition of CO₂ gas from the Lassen geothermal system is shown as a triangle (7). Circles correspond to samples from large springs (>0.3 m³ s⁻¹), solid diamonds indicate samples from smaller springs (<0.3 m³ s⁻¹), and open squares represent surface waters.

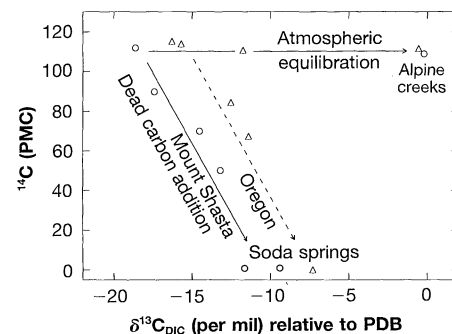
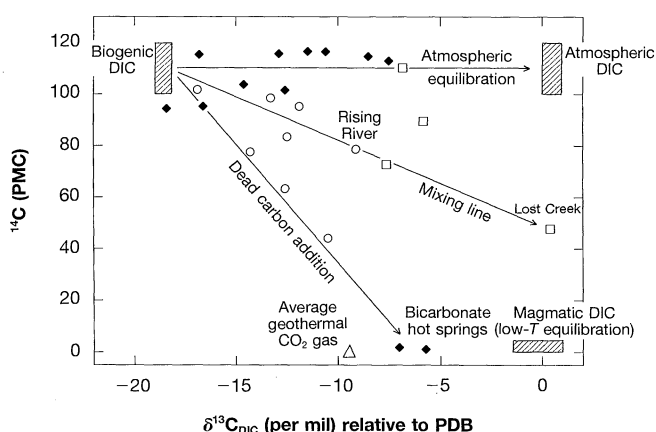


Fig. 3. Variations in ¹⁴C versus δ¹³C values of DIC in waters from Mount Shasta (circles) and southern Oregon (triangles). Mixing processes are indicated by lines. Biogenic and atmospheric DIC end-members are inferred to be compositionally similar to the Lassen system (see Fig. 2), whereas the magmatic DIC end-member is represented by soda springs.

ence of HCO_3^- hot springs in the geothermal system. In contrast, the composite volcanoes that make up most of the Cascade Range evidently lack the Lost Creek type of low- ^{14}C water, suggesting a low rate of diffuse CO_2 flux in these systems. Soda springs rich in CO_2 associated with composite volcanoes are situated only at low elevations, on the margins of the volcanoes. The stratified lithology of these volcanoes may therefore provide an effective barrier to diffuse CO_2 emissions on the volcanic edifice.

In the Lassen region, sufficient data exist to construct a generalized ground-water ^{14}C contour map (Fig. 4). The contour lines are based primarily on data from the thermal and large-volume springs. Dashed contour lines encompass the entire Lassen geothermal area (shaded regions) under the assumption that low- ^{14}C fluids discharge throughout this region. The elongate, concentric pattern of contours (Fig. 4) stretches from Lassen Peak northward toward Rising River Springs. Radiocarbon values gradually increase along this flow path as low- ^{14}C ground water from the Lassen Peak region

mixes with water enriched in biogenic DIC, yielding a final mixed composition like that of Rising River. Two springs with modern or near-modern ^{14}C values (104 and 94 PMC) occur near Lassen Peak (Fig. 4), in close proximity to samples with much lower ^{14}C values. Heterogeneous ^{14}C values may reflect local variations in ground-water flow paths. Shallow, localized flow paths with short aquifer residence times will tend to limit ground-water interaction with diffuse magmatic CO_2 emissions, as compared with deeper flow paths in the same region.

We infer that most of the dissolved magmatic carbon in the Lassen region originates from diffuse CO_2 emissions, particularly in view of the fact that the Lassen geothermal system is centered south of the regional drainage divide, opposite the dominant ground-water flow system. Although small geothermal vents occur on the north side of Lassen Peak (16), they cannot account for the quantity of magmatic carbon present in the large-volume springs. Additional evidence for diffuse CO_2 emissions is provided by data from a large spring located ~ 20 km west-northwest of Lassen Peak. This spring has a ^{14}C value of 78 PMC (Fig. 4) and a $\delta^{13}\text{C}$ - ^{14}C pair that plots on the "dead carbon addition" line of Fig. 2. However, its $\delta^{18}\text{O}$ value indicates meteoric recharge from the north, thus ruling out any direct connection with the Lassen Peak highlands.

Given a combination of known discharge rates, DIC concentrations, and ^{14}C activities for major flow systems, it is possible to estimate the dissolved magmatic carbon flux for any given volcanic center. We have calculated approximate flux values for both the Lassen and Mount Shasta volcanic centers (Table 1). The Lassen data include the three largest low- ^{14}C springs and one creek, all of which are located north of Lassen Peak. We determined the fraction of magmatic DIC in each water, assuming two-component ^{14}C mixing between magmatic (0 PMC) and biogenic-atmospheric sources (110 PMC). Using this approach, we estimate a minimum dissolved magmatic carbon flux of 1.1×10^7 kg year $^{-1}$ at Lassen. If all of the dissolved magmatic carbon is in the form of HCO_3^- , this is equivalent to 7.6×10^6 kg year $^{-1}$ of magmatic CO_2 gas. Published gas chemistry data (15) and mass flux estimates (16) for the Lassen geothermal system indicate a CO_2 gas effusion rate of 3.5×10^7 kg year $^{-1}$ (18). This result suggests the dissolved magmatic carbon flux is equivalent to $\sim 20\%$ of the estimated geothermal CO_2 gas flux at Lassen.

Our dissolved magmatic carbon flux estimate for the Mount Shasta region is based on the ^{14}C values of the two major river systems that drain the area, the Sacramento and McCloud rivers (Fig. 1). The majority

of the spring flow from Mount Shasta is contributed to these rivers. Two independent dissolved magmatic carbon flux determinations for the Sacramento River varied by $<10\%$, despite significantly different flow conditions. The McCloud River exhibits only small variations between base flow and peak runoff conditions because virtually the entire discharge is contributed by one group of springs. A ^{14}C measurement of these springs (Big Springs of the McCloud River) was similar to the integrated value for the river (Table 1). The total dissolved magmatic carbon flux for these two rivers is estimated at 1.2×10^7 kg year $^{-1}$, equivalent to 8.5×10^6 kg year $^{-1}$ of magmatic CO_2 gas. This value is slightly larger than the dissolved magmatic carbon flux from Lassen. However, geothermal activity at Mount Shasta is very limited, consisting of one small group of acid-sulfate springs located near the summit (19). The lack of a large, observed gaseous CO_2 flux suggests either that the total magmatic CO_2 flux is lower at Mount Shasta than at Lassen or that a comparable magmatic flux at Mount Shasta is unaccounted for. In the latter case, the soda springs that occur at Mount Shasta and in Oregon, but not at Lassen, may represent deep ground water from beneath these composite cones that buffers the unaccounted CO_2 by water-rock interaction.

REFERENCES AND NOTES

- J. C. Baubron, P. Allard, J. P. Toutain, *Nature* **344**, 51 (1990); P. Allard *et al.*, *ibid.* **351**, 387 (1991); S. Anza *et al.*, *Acta Vulcanologica* **3**, 189 (1993); C. D. Farrar *et al.*, *Nature* **376**, 675 (1995); S. Giannamano, S. Gurrieri, M. Valenza, *Bull. Volcanol.* **57**, 52 (1995).
 - T. M. Gerlach, *Eos* **72**, 249 (1991); J. C. Varekamp, R. Kreulen, R. P. E. Poorter, M. J. Van Bergen, *Terra Nova* **4**, 363 (1992); S. N. Williams, S. J. Schaefer, M. L. Calvache, D. Lopez, *Geochim. Cosmochim. Acta* **56**, 1765 (1992).
 - P. Allard, D. Dajilevic, C. Delarue, *J. Volcanol. Geotherm. Res.* **39**, 195 (1989); W. F. Giggenbach, Y. Sano, H. U. Schmincke, *ibid.* **45**, 311 (1991).
 - A. P. McNichol, G. A. Jones, D. L. Hutton, A. R. Gagnon, R. M. Key, *Radiocarbon* **36**, 237 (1994).
 - The ^{14}C values were determined at the Lawrence Livermore National Laboratory Center for Accelerator Mass Spectrometry. Analytical precision is ± 1 PMC. The $\delta^{13}\text{C}$ values were measured on a conventional gas-ratio mass spectrometer and have an analytical precision of ± 0.3 per mil.
- $$\delta^{13}\text{C} = \left[\frac{(^{13}\text{C}/^{12}\text{C})_{\text{unk}}}{(^{13}\text{C}/^{12}\text{C})_{\text{std}}} - 1 \right] \times 1000$$
- where unk refers to the carbon ratio of the sample and std refers to the carbon ratio of a PDB standard, and units are per mil.
- W. G. Mook, J. C. Bommerson, W. H. Staverman, *Earth Planet. Sci. Lett.* **22**, 169 (1974); W. G. Mook, *Neth. J. Sea Res.* **20**, 211 (1986).
 - C. J. Janik, N. L. Nehring, A. H. Truesdell, *Trans. Geotherm. Res. Council* **7**, 295 (1983).
 - I. Barnes, R. W. Kistler, R. H. Mariner, T. S. Presser, *U.S. Geol. Surv. Water-Supply Pap.* **2181** (1981).
 - J.-L. Join and J. Coudray, *Geodinamica Acta (Paris)* **6**, 243 (1993).
 - S. E. Rantz, *U.S. Geol. Surv. Basic Data Compil.*, isohyetal map, scale 1:1,000,000 (1969).

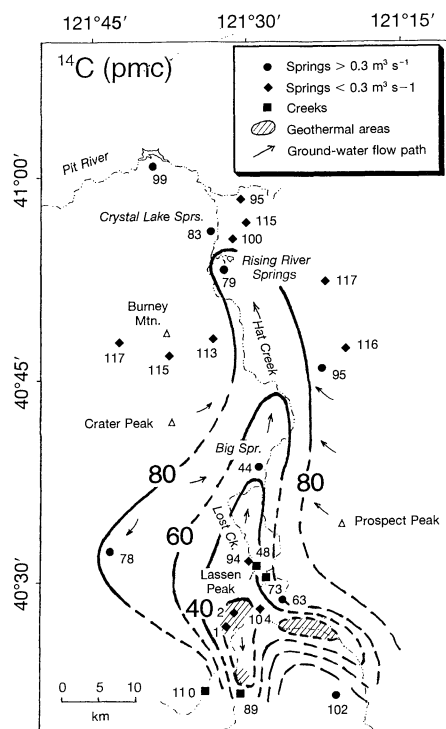


Fig. 4. Radiocarbon contour map of ground water in the Lassen region of northeastern California. Contour lines are controlled primarily by data from large springs (circles), which represent deep ground-water flow paths (arrows). Contours are dashed where inferred. Shaded areas correspond to regions of hot spring activity. Numbers next to sample locations indicate ^{14}C values (PMC). Locations are noted for major springs and creeks used to estimate the regional dissolved magmatic CO_2 flux (see Table 1).

11. A similar process is described by D. K. Solomon and T. E. Cerling, *Water Resour. Res.* **23**, 2257 (1987).
12. T. P. Rose, M. L. Davissou, R. E. Criss, *J. Hydrol.* **179**, 207 (1996).
13. I. Levin *et al.*, in *Radiocarbon After Four Decades: An Interdisciplinary Perspective*, R. E. Taylor, A. Long, R. S. Kra, Eds. (Springer-Verlag, New York, 1992), pp. 503–518.
14. C. D. Keeling *et al.*, *Geophys. Monogr. Am. Geophys. Union No. 55* (1989), pp. 165–236.
15. L. J. P. Muffler *et al.*, in *Proceedings of the Pacific*

- Geothermal Conference* (Auckland, New Zealand, 8 to 12 November 1982) (University of Auckland, Auckland, New Zealand, 1982), pp. 349–356.
16. M. L. Sorey and E. M. Colvard, *U.S. Geol. Surv. Water Res. Invest. Rep. 94-4180-A* (1994).
17. M. A. Clyne, *J. Geophys. Res.* **95**, 19651 (1990).
18. The vapor-dominated geothermal reservoir at Lassen has a H₂O/gas ratio of 85 and a gas phase that contains 92.7 mol % CO₂ (15). The bulk CO₂ concentration in the steam discharge is therefore 2.67% by weight. The estimated steam discharge rate from

the geothermal system is 41 kg s⁻¹ (16). This implies a CO₂ flux of 1.1 kg s⁻¹ or an annual flux of 3.5 × 10⁷ kg year⁻¹.

19. H. Williams, *Z. Vulkanol.* **15**, 225 (1934).
20. We thank R. E. Criss and two anonymous reviewers for comments and suggestions. This work was performed under the auspices of the U.S. Department of Energy by Lawrence Livermore National Laboratory under contract W-7405-Eng-48.

13 May 1996; accepted 17 July 1996

Fossil Velvet Worms in Baltic and Dominican Amber: Onychophoran Evolution and Biogeography

George Poinar Jr.

Velvet worms identified in Baltic and Dominican amber demonstrate that terrestrial onychophorans were present in the early Tertiary. Characters of the amber fossils are similar to those of the Cambrian *Aysheaia* and the Pennsylvanian *Helenodora*, which suggests that these Paleozoic lobopods are ancestral to extant velvet worms. The presence of slime secretions in the Dominican amber fossil shows that the slime gland-pore complex had developed by the mid-Tertiary and could have been an adaptation to terrestrial life. The Baltic amber fossil shows that the range for this now predominately gondwanan group was expanded in the Tertiary.

Members of the phylum Onychophora or velvet worms have incited debate for years regarding their position in the animal kingdom (1). Traditionally they have been regarded as a sister group to the monophyletic Arthropoda and a link between the Annelida and the Arthropoda, with the Cambrian *Aysheaia* possibly representing an ancient marine ancestor of today's velvet worms and of the entire Atelocerata (Myriapoda and Hexapoda) (2). However, there had not been any intermediate forms connecting the Cambrian *Aysheaia* and *Xenusion* (3–5), and Pennsylvanian *Helenodora* from (6), to present-day onychophorans.

Here, I describe terrestrial velvet worm fossils found in Dominican and Baltic amber and discuss their connection to Paleozoic forms (3, 7) and extant onychophorans. In addition, I will discuss the development of the elaborate slime gland-pore complex found in modern velvet worms, and the implications the Baltic amber fossil has regarding the distribution of onychophorans in the past.

The purple- to black-colored Baltic amber specimen (about 40 million years) (8) (Fig. 1) is represented by 8 mm of the anterior of the body. It contains a pair of antennae and nine pairs of legs. The brownish-tan-colored Dominican Republic amber specimen (20 to 40 million years) (8) (Fig. 2) is represented by 4.38 mm of the anterior of the body. The Dominican amber specimen bears a pair of antennae, oral papillae, and 19 pairs of legs.

One character that connects the two

amber fossils with the Paleozoic forms is the structure of the legs (sac-like, nonjointed extensions of the body). The leg of a typical present-day onychophoran consists of a proximal trunk portion and a dorsal foot portion bearing a terminal pair of claws and associated papillae. In the amber fossils, the foot is lacking and only the trunk is present (Figs. 1 to 3). The claws of the Dominican fossil are attached to the trunk, a condition similar to that reported in *Aysheaia pedunculata* (3) and *Helenodora* (6). This undifferentiated type of leg structure is also reminiscent of that found in some Tardigrada (*Haplomacrobotus*) (9). A similarity be-

tween *Aysheaia* and tardigrades has already been proposed (10).

One of the unique characters (and certainly essential for survival) of extant onychophorans is the slime gland and pore complex (1). The slime glands are well developed in relation to the body size of velvet worms. These glands open to the exterior at the oral or slime papillae and produce a water-soluble sticky secretion that is used both to obtain food and for defense. There is no definite evidence of oral papillae in the two species of *Aysheaia* or in *Helenodora*. Slime would have been ineffective in an aquatic environment, and these organs evolved as the animal adapted to terrestrial life (11). The oral papillae are quite distinct in the Dominican amber specimen, and a thick, copious deposit extends from near the openings of each gland (Fig. 3). This deposit is interpreted as slime that had been emitted from the oral papillae as a triggered defense reaction at the time the animal fell into the sticky resin. This fossil establishes a minimum time for the evolution of this slime production system and connects the Dominican fossil to the modern velvet worms.

If the slime gland-pore complex did evolve as an adaptation to invasion of the land, then its primary function (aside from a possible use as a protective coating as the animal became terrestrial) was probably for



Fig. 1. Lateral view of a fossil onychophoran in Baltic amber (body = 8 mm).



Fig. 2. Lateral view of the right side of a fossil onychophoran in amber from the Dominican Republic (body = 4.38 mm).

Department of Entomology, Oregon State University, Corvallis, OR 97331, USA. E-mail: poinar@bcc.orst.edu